

Thermal Analysis of Sheet Metal During Ultrasonic Welding



P. Ravikiran

**M.Tech (Thermal Engineering),
Department of Mechanical
Engineering,
Sri Vaishnavi College of
Engineering, Srikakulam.**



Suresh Babu Sattaru

**Assistant Professor,
Department of Mechanical
Engineering,
Sri Vaishnavi College of
Engineering, Srikakulam.**



Pondrati Padmavathi

**Assistant Professor,
Department of Mechanical
Engineering,
Sri Vaishnavi College of
Engineering, Srikakulam.**

ABSTRACT:

Welding is the process of joining two components by means of thermal energy, with or without applying the application of pressure. It is the alternative method for casting or forging and as a replacement of bolted and rivets joints. But in our case the ultrasonic welding is used for welding the materials. So the distribution of residual stress in welded joint of high strength steel material was investigated by means of finite element method (FEM) by using Ansys software. In this analysis the pressure is applied between two plates. Due to the friction between the plates the thermal energy is developed.

This energy is used to join the two plates by means of heat flux. The heat flux is nothing but the concentration of heat on the surface area. So that the two dimensional drawing of ultrasonic welding setup is modeled in the Ansys workbench environment. Then the heat flux is applied between contact areas of the two plates. In this analysis the welding process is assumed as time being process. Because the temperature will increased with respect to the time. So that transient analysis is made and the results were obtained.

INTRODUCTION

1.1 ULTRASONIC WELDING:

Ultrasonic metal welding (USMW) was invented over 50 years ago and has now been in use in industry for many years.

USMW is a process in which two metals are joined by the application of ultrasonic vibrations, under moderate pressure, in which the vibrations are applied parallel to the interface between the parts. The high frequency relative motion between the parts forms a solidstate weld through progressive shearing and plastic deformation between surface asperities that disperses oxides and contaminants and brings an increasing area of pure metal contact between, and bonding of, the adjacent surfaces.

1.2 Ultrasonic Metal Welding:

Ultrasonic metal welding (USMW) is used in many fields like automotive, shipbuilding, architectural industries and brazing in electronic components manufacture. Ultrasonic can be used to weld different metals together, without solder and flux or special preparation. The process is different from plastic welding in that the two components are vibrated parallel to the interface as shown in fig.1. Ultrasonic metal welding consists of fundamental parts.

1. The electrical part
2. The electromechanical transducer
3. The mechanical part

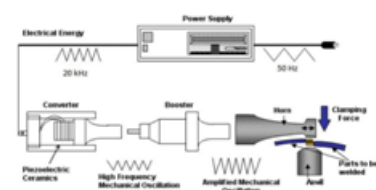


Fig1. Illustration of ultrasonic metal welding system

1.4 PRINCIPLES OF ULTRASONIC METAL WELDING

The application of ultrasound to metal joining, for improving grain refinement of fusion welds, and for brazing and soldering, dates back over 60 years. The first steps to the discovery of ultrasonic metal welding (USMW) “as we now know it” occurred in the late 1940’s when, in research at the AeroProjects Company of West Chester, Pennsylvania (the forerunner of the current Sonobond Corporation), ultrasonic vibrations were applied to conventional resistance welding equipment, with the objective of decreasing surface resistance in spot welding of aluminums [2]. In the course of this work, it was discovered that ultrasound alone was capable of producing a bonding of the metals. Initial equipment used a longitudinal mode of vibration to the work pieces, similar to that used today for ultrasonic plastic welding. Further study showed that lateral vibration components of the sonotrode were in fact responsible for the traces of bonding observed in the parts. Added development was aimed at enhancing this transverse vibration, and led, by the mid- 1950, to both the wedge-reed and lateral drive configurations now in use. Extensive research efforts spread to other laboratories in the United States by the late 1950’s, and soon after that, research groups throughout the world, but especially in the (former) Soviet Union, initiated efforts.

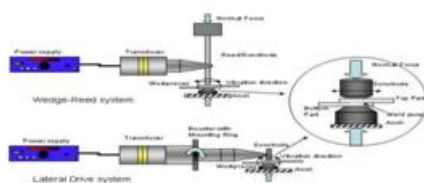


Fig2. Wedge-Reed and Lateral Drive ultrasonic welding systems

LITERATURE REVIEW:

P. Jedrasiak, H.R. Shercliff, Y.C. Chen, L. Wang, P. Prangnell, and J. Robson's paper is about Modelling of the Thermal Field in Dissimilar Alloy Ultrasonic Welding. This paper describes a finite element model for predicting the temperature field in high power ultrasonic welding aluminum AA6111 to two

dissimilar alloys, magnesium AZ31, and low carbon steel DC04. Experimental thermocouple and other evidence are used to infer the magnitude and distribution of the heat input to the workpiece, as a function of time, for each of the material combinations welded. The resulting temperature histories are used to predict the growth of intermetallic phases at the interface in Al-Mg welds. The microstructural model successfully predicts the thickness of the intermetallic layer, but the sensitivity of the results to temperature is demonstrated. Vijay Singh pal, Pavan Agrawal's study is Analysis of Bonding Strength of Ultrasonic Welding Process. In ultrasonic welding, high frequency vibrations are combined with pressure to join two materials together quickly and securely. Ultrasonic welding can join dissimilar metals in a split second, ultrasonic welding eases problematic assembly and this cost effective technique may be key to massproducing fuel efficient.

In this work effect of various parameters on weld strength have been studied. Welding of .5 mm aluminium plates were successfully welded by 20 kHz ultrasonic welding system. One dimensional vibration system for ultrasonic lap spot welding of metal plate of aluminium have studied. The relationships between weld strength and the variables of weld energy, duration of weld cycle, have studied Experiment was carried out to determine the mechanism of aluminium-aluminium plate bonding. These experiment, including effect of amplitude and pat tern of bond formation. Experiment was carried to find out the optimum parameter for maximum strength. BOKKA.RAVI KIRAN, K.Gowri Sankar did a review on THERMAL ANALYSIS OF DISSIMILAR METAL WELDING PROCESS IN LASER WELDING. laser welding process has successfully used for joining of dissimilar metals i.e. copper and steel. The distribution of the temperature field in laser welding using copper and stainless steel sheets was simulated by ANSYS 16. The thermal properties are used for thermal simulation and the. Traveling heat heat flux model is used to simulate and observe the simulated thermal effects in the several welding joints like butt, lap, edge and t

At the joints the temperature are applied to the joints of the two dissimilar metals the temperature distribution of over the joints is observed and recorded in order to improve the welding process and temperature distribution over the joints. The joints are designed in the solid works and simulated the process in the ANSYS transient thermal the graphs and results are noted after simulation. This work undergoes the basic simulation process and theoretical formulations and software skills to design and simulate the thermal distribution.

AIM:

The objectives of this study are

1. To simulate the temperature distribution at weld interface, sonotrode and anvil during ultrasonic welding of metallic materials (aluminum alloy).
2. To simulate the stress distribution in the joint and sonotrode during USMW.
3. To simulate the temperature distribution for varying work piece thickness, and surface properties (coefficient of friction). These simulations are done using ANSYS.
4. To study the effect of clamping force, weld time, material thickness and coefficient of friction on temperature at the interface and HAZ by simulation.

When new metals and weld conditions are encountered and they pose difficulties in achieving quality welds, a study of this nature can provide a direction for the researchers to proceed towards optimum values of parameters. In this work, aluminum is considered as a work piece.

Modeling of temperature distribution:

Modeling of temperature distribution in weld interface of work piece is attempted in this study. Two-dimensional rectangular co-ordinate systems (x, y) are used for formulating the problem because of the work piece geometry.

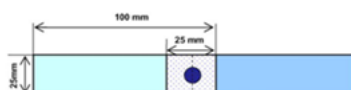


Fig. 1 – Standard specimen (weld coupon).

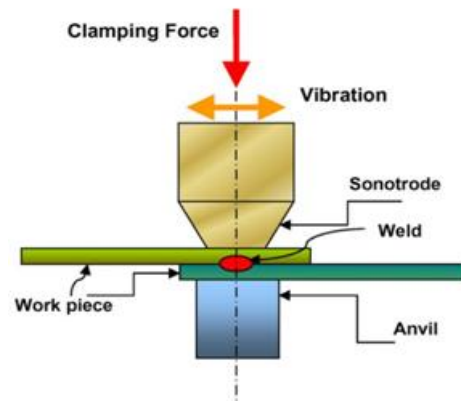


Fig. 2 – Schematic representation of weld interface in ultrasonic metal welding

The partial differential equation governing heat transfer in axis-symmetric geometry is given by:

$$K \left(\frac{\partial^2 T}{\partial x^2} + \frac{\partial^2 T}{\partial y^2} \right) + Q - \rho \frac{\partial T}{\partial t} = 0$$

The standard weld coupon used for USW (Welding Handbook, 1964) in Fig. 1 is same as that for resistance spot welding. The following assumptions are made in simulating the temperature distribution using ANSYS 15.0.

- I. The sonotrode that was used in this analysis had a uniform cross-sectional area (circular) at the tip.
- II. There was no air gap between the two aluminum sheets (perfect contact).
- III. At the end of the weld, the area of the sonotrode AS will be equal to the area of the deformation zone ADZ and will be equal to the area of the weld AW (AS = ADZ = AW).
- IV. The room temperature is assumed to be uniform and it is taken as 30 °C.

The material properties considered were coefficient of thermal conductivity (k) specific heat (c) and density (ρ) for performing thermal analysis. Young’s modulus, Poisson’s ratio and coefficient of thermal expansion were considered for performing structural analysis.

The properties of the materials (ASM Handbook vols. 1 & 2, 1990 and 1998) used for sonotrode, work piece and anvil are listed in Table 1.

S.NO.	MATERIAL	THERMAL CONDUCTIVITY (W/M°C)	SPECIFIC HEAT (J/Kg°C)	DENSITY (KG/M ³)	YOUNG'S MODULUS (GPa)	POISSON'S RATIO	THERMAL EXPANSION COEFFICIENT(1/°C)
1	STEEL(SONOTRODE AND ANVIL)	24.3	460	7800	210	0.3	1.51E-05
2	ALUMINUM (WORK PIECE)	183	896	2700	70	0.35	2.43E-05
3	COPPER (WORK PIECE)	393	385.2	8900	117	0.3	1.66E-05
4	polyamide-6 (WORK PIECE)	0.24	170	960	2.3	0.29	9.50E-05

Heat generation and conduction at the weld:

During USMW heat is generated at the weld interface and the surrounding area as well as at the sonotrode top surface owing to plastic deformation and friction. Fig. 2 shows the situation in the USMW. This generation of heat and the subsequent change of temperature have a significant impact on the properties of the welded joint. It was observed that in the initial phase of welding, plastic deformation occurs at the interface between sonotrode and work while the knurls on the sonotrode engage into the top surface of part. By this, heat is generated as well.

But it was found that a typical welding cycle is 20–25 times longer than the initial phase. Therefore, this initial heating phase at the sonotrode has been neglected. For practical purposes the heat input due to plastic deformation and due to friction has been separated. The heat input due to plastic deformation has been confined to the deformation zone area (i.e. the sonotrode area AS in this model) and the heat input due to friction is confined to the friction area AFR surrounding the weld area.

Heat Generation Due to Deformation:

To model the heat input into the parts and temperatures that occur during welding one has to take a closer look at the distribution of the heat sources across the deformation zone and their development during the weld cycle. At the beginning of the weld cycle the deformation islands occur randomly across the deformation zone. Because of the high thermal conductivity of aluminum the temperature will even out very rapidly across the deformation zone. From this it is understood that the total power developed in all deformation islands is distributed evenly over the

entire volume of the deformation zone. Heat generation due to deformation (De Vries, 2004) is the power dissipated over the weld area. Power at the weld area (Eq. (2)) depends on the weld force (Eq. (3)) which is a function of yield strength and clamping

$$Q_w = \frac{P_{Total}}{A_w} = \frac{F_w \times V_{avg}}{A_w} \quad (2)$$

Weld force is given by

$$F_w = \sqrt{\left(\frac{Y_T}{2}\right)^2 - \left(\frac{F_N/A_{DZ}}{2}\right)^2} \times A_{DZ} \quad (3)$$

$$\text{Average sonotrode velocity } V_{avg} = 4 \times \xi_0 \times f_w \quad (4)$$

Heat flux due to deformation is given by using Eq's (2)-(4)

$$Q_w = \frac{\sqrt{(Y_T/2)^2 - (F_N/A_{DZ})^2} \times A_{DZ} \times 4 \times \xi_0 \times f_w}{A_w} \quad (5)$$

At the end of the weld time, area of the deformation zone ADZ will be equal to the area of the weld AW. Applying the limit condition in Eq. (5) the heat flux due to deformation will become

$$Q_w = \sqrt{(Y_T/2)^2 - ((F_N/A_{DZ})/2)^2} 4 \times \xi_0 \times f_w \quad (6)$$

Variation of yield strength depends upon the temperature (in Eq. (7)) is found out experimentally by De Vries (2004) and is shown in Fig. 3. The average temperature dependent yield strength can be found by

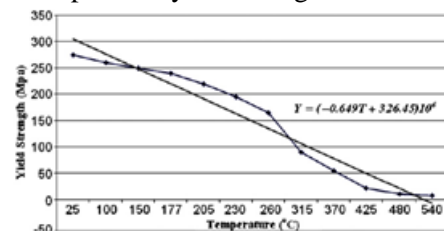


Fig. 3 - Variation of yield strength with temperature (De Vries, 2004)

$$Y_T = \frac{\int_0^{750} (-0.649T + 326.5) \times 10^6 dT}{\Delta T}$$

$$= \frac{[((-0.649T^2/2) + 326.5T) \times 10^6]_0^{750}}{\Delta T}$$

$$= 83.125 \times 10^6 \text{N/m}^2$$

Heat flux due to deformation for a clamping force of 1600N is given by

$$Q_w = \sqrt{\left(\frac{83.125}{2}\right)^2 - \left(\frac{1600/20 \times 10^{-6}}{2}\right)^2} \times 4 \times 13$$

$$\times 10^{-6} \times 20000$$

$$= 11.288 \times 10^6 \text{W/m}^2$$

Heat generation due to friction:

Frictional area of welding zone is twice than the radius of deformation zone area (De Vries, 2004) which is shown in Fig. 4. Since the heat input through friction takes place only outside the weld area. The area involved in friction is given by

$$A_{FR} = A_R - A_W \tag{8}$$

The power can be calculated as the product of frictional force (FFR) and the average speed. This flux is dissipated by frictional force.

$$Q_{FR} = \frac{P_{FR}}{A_{FR}} = \frac{F_{FR} \times V_{avg}}{A_{FR}} \tag{9}$$

Frictional force is given by

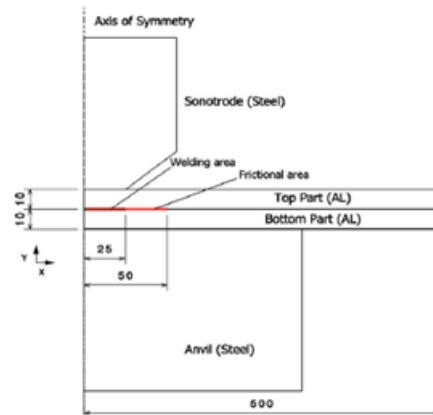
$$FFR = \mu \times FN \tag{10}$$

Using Eqs. (10) and (4) in Eq. (9) heat flux due to friction is

$$Q_{FR} = \frac{\mu \times FN \times 4 \times \xi_o \times f_w}{A_{FR}} \tag{11}$$

$$Q_{FR} = \frac{0.3 \times 1600 \times 4 \times 13 \times 10^{-6} \times 20000}{60 \times 10^{-6}}$$

$$= 8.32 \times 10^6 \text{W/m}^2$$



Initial Condition:

T(X,Y,0) = T0 = Room temperature

Boundary conditions:

Q(Convection) is the heat lost due to convection to the surroundings from lateral surfaces of area A with overall heat transfer coefficient (Nijaguna, 2005) (h) of 5 J/(m2 °C).. where Q(FW) and Q(FR) are the heat fluxes generated due to deformation and heat flux generated due to friction in W/mm2, respectively.

Q(FW) and Q(FR) were calculated for different clamping forces, and different coefficients of friction. The contact resistance of the faying surface is a function of load, temperature and average yield strength in contact materials.

A 2D six-noded triangular thermal solid (plane 55) element is used for performing thermal analysis. The mesh size chosen was fine and contact is established between sonotrode with top work piece, top work piece with bottom work piece, and bottomwork piece with anvil.

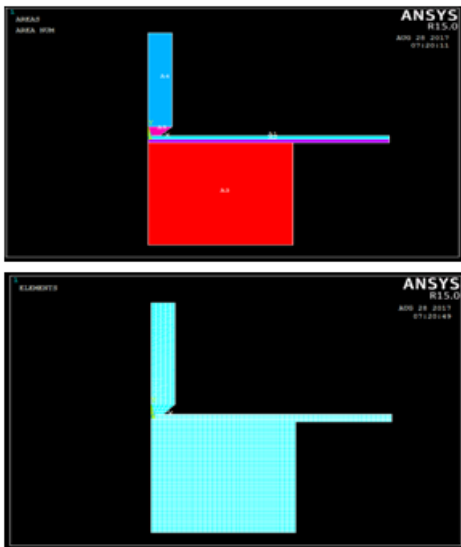
The heat flux due to deformation was applied in sonotrode area (20mm2) and the heat flux due to friction was applied in frictional area (60mm2). Convection was applied on the boundaries of the work piece that is not in contact with the sonotrode and anvil which is shown in fig and reference temperature was taken as 30°C. The transient analysis was carried out with time steps of 0.1 s.

Modelling of stress distribution:

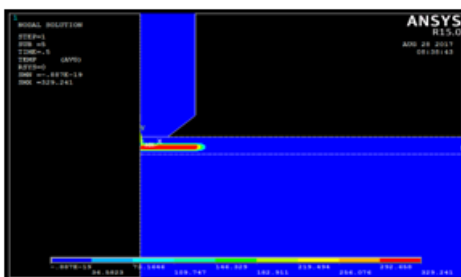
A 2D six-node triangular structural solid (plane 2) element was selected for structural analysis. The forces are applied on the nodes of the sonotrode which is in contact with the work piece. The displacements of the anvil were arrested. The boundary conditions and the pre-processor for performing structural analysis are shown in Fig. 6. The clamping forces were applied on the nodes and the displacement of the anvil is made as zero. Analysis type selected was transient with time steps of .001 for 0.5 s. The simulation was performed for different clamping forces, different values of thickness and different coefficients of friction. The results obtained in the thermal and structural analyses are presented in the next section.

Ansys Results:

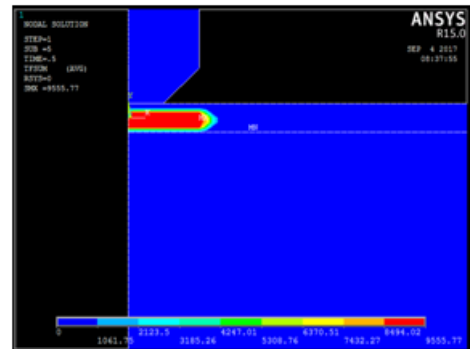
Ansys Model:



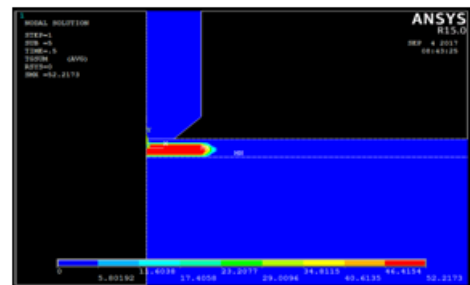
CASE 1: ALLUMINIUM MATERIAL



Temperature distribution plot with maximum temperature generated is 3290C

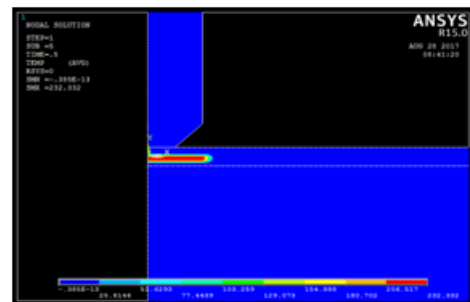


Heat flow through material aluminium is 9555 (0C/mm2)

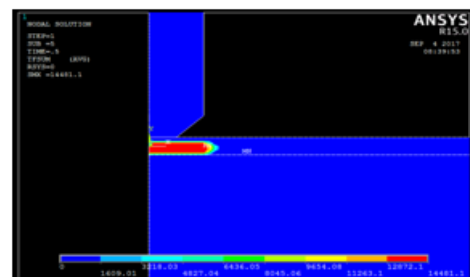


Thermal Gradient for Aluminium 52

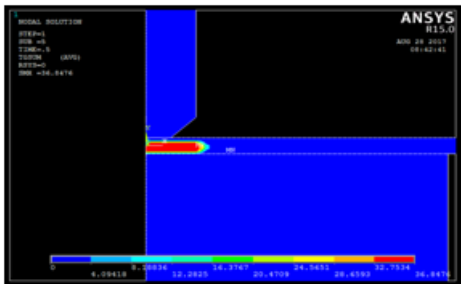
Case 2: Copper Material



Temperature distribution plot with maximum temperature generated is 2320C



Heat flow through material Copper is 14481 (0C/mm2)

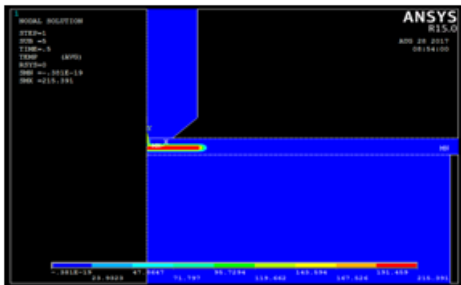


Thermal Gradient for Copper 36

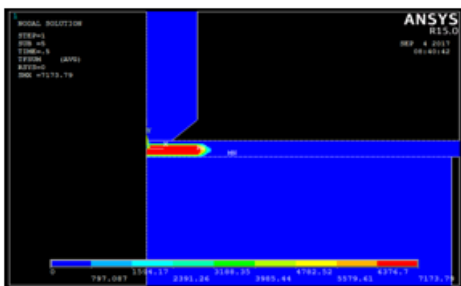
RESULT TABLE:

S.NO.	MATERIAL	TEMPERATURE (°C)	HEAT FLOW	THERAL GRADIANT
1	ALUMINUM (WORK PIECE1)	329	9.50E+03	52
2	COPPER (WORK PIECE2)	232	1.44E+04	36
3	polyamide-6 (WORK PIECE2)	215	7.10E+03	34

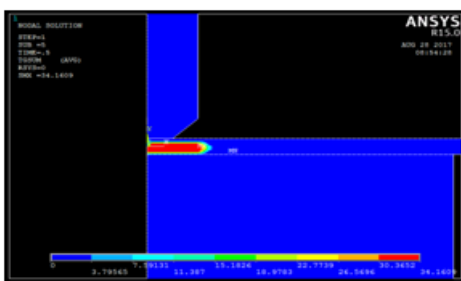
Case 3: Polyamide-6 Material



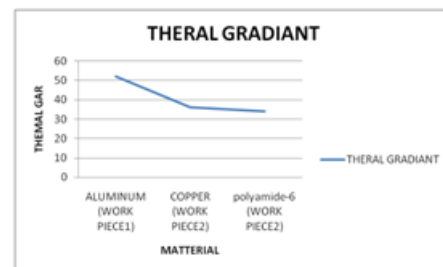
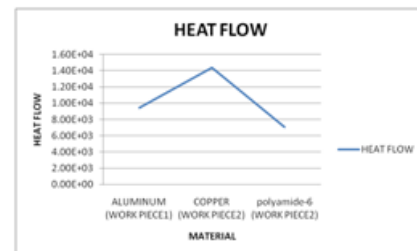
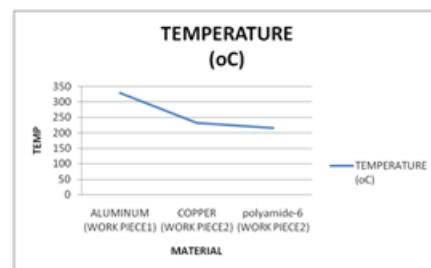
Temperature distribution plot with maximum temperature generated is 215°C



Heat flow through material Polyamide-6 is 7173 (0C/mm2)



Thermal Gradient for Polyamide-6 34



MATLAB CODING:

```

% All the equations use dimensionless x and y.
myconst;
inc=0.01;
nod=100;
nop=nod+1;
L= 0;
for L = 1:nop
mu2(L)=5000+10*(L-1); % Input in Pa-s
mu(L)=mu2(L)*101.972; % Unit conversion to glm-s
for l=1 :nop
dlx(l)=(l-1)*inc;

```

```
warning off MATLAB:fzero:UndeterminedSyntax;
options=[ ];
del(I)=fzero('HAZfunc',I,options, dlx(I),mu(L)); %
Find the thickness ofHAZ
end
for I=1:nop
F(I)=int( dlx(I),del(I),mu(L));
end
% first integral of P using simpson's mIe
for I=1:nop
sum1 =0; sum2=0;
for x1 = 1+2 : 2 : nop-2
sum1 = sum1+F(x1);
end
for x2 = 1+1 : 2 : nop-1
sum2 = sum2+F(x2);
end
P(I) = inc/3*(F(I)+F(nop)+ 2*sum1 + 4*sum2);
end
sum3=0; sum4=0;
for x1 = 3 : 2 : nop-2
sum3 = sum3+P(x1);
end
for x2 = 2 : 2 : nop-1
sum4 = sum4+P(x2);
end
% second integral ofP using simpson's mIe
Pv(L) = inc/3*(P(1)+P(nop)+ 2*sum3 + 4*sum4); %
The output Pressure is in unit of
glml\2
Pv2(L)= Pv(L) * 1 e-61101.972; % Unit conversion of
the resulting pressure to MPa
end
L=1:nop;
plot(Pv2(L)', mu2(L)')
xlabel('Estimated welding pressure (MPa)')
ylabel('Melt average viscosity (Pa s)')
title ('Estimate melt average viscosity')% All the
equations use dimensionless x and y.
mu2 = 11090;
mu = mu2*101.972;
myconst;
inc=0.01;
nod=100;
```

```
nop=nod+1;
for 1=1:nop
dlx(1)=(I-1)*inc;
% Input in Pa-s
warning off MA TLAB :fzero: UndeterminedSyntax;
options=[ ];
del(I)=fzero('HAZfunc',I,options, dlx(1),mu); % Find
the thickness ofHAZ
end
forI=1:nop
F(I)=int( dlx(1),del(1),mu);
end
% first integral of P using simpson's mIe
for 1=1 :nop
sum 1 =0; sum2=0;
for x1 = 1+2: 2 : nop-2
sum1 = sum1+F(x1);
end
for x2 = 1+1 : 2 : nop-1
sum2 = sum2+F(x2);
end
P(I) = inc/3*(F(I)+F(nop)+ 2*sum1 + 4*sum2);
end
sum3=0; sum4=0;
for x1 = 3 : 2 : nop-2
sum3 = sum3+P(x1);
end
for x2 = 2 : 2 : nop-1
sum4 = sum4+P(x2);
end
% second integral ofP using simpson's mIe
Pv = inc/3*(P(1)+P(nop)+ 2*sum3 + 4*sum4);
1=1 :nop;
subplot(2,2,1.5)
plot( dlx(1)',del(1)* 1 e6')
xlabel('Dimensionless x')
ylabel('Thickness (micrometer)')
title ('Fluid film thickness')
J=0;
for J = 1:nop
dly(J)=(J -1)*inc;
end
forI=1:nop
for J=1:nop
```

```
Tv(I,J) = DelT(dlx(I),dly(J),del(I),mu);
end
end
for I=1:nop
for J=1:nop
ShearS(I) = Shear(del(I),mu)/101.972;
SqueezeS(I,J) = Squeez(dlx(I), dly(J),
del(I),mu)/101.972;
end
end
% Plot the resulting temperature profile vs
dimensionless x, y
I=1:nop;
J=1:nop;
subplot(2,2,3)
mesh(dlx(I)', dly(J)', Tv(I,J))
xlabel('Dimensionless x'), ylabel('Dimensionless y'),
zlabel('T -Tm( oC)')
title ('Temperature Profile')
function y = HAZfunc(del,dlx,mu)
myconst;
y = d*ml*vO*de1A3/(2*mu)-N'2*deIA2/4-
3*vQl'2*bA2*dlxA2/2;
function y=DeIT( dlx,dly,deI,mu)
myconst;
y=muJk*«9*vOA2*bA2/deIA2*dlxA2)*(dly/6-
dlyA2/2+2*dlyA3/3-dlyA4/3)+AA2/4*(dlydlyA2));
function y = Shear (del,mu)
myconst;
y = 4*a*f*mu/del;
function y = Squeeze (dlx, dly, deI, mu)
myconst;
y = 3*vO*b*mu*dlx*(1-2*dly)/de1A2;
function y=int( dlx,del,mu)
myconst;
y=3*mu*vO*bA2*dlx/deIA3;
```

CONCLUSION:

Main results obtained from the above study are- With increase in amplitude the failure load is decreasing or we can say that the

- weld strength or tensile strength is decreasing. At moderate weld pressure, failure load or tensile stress is minimum.

- At low or moderate weld time failure load is maximum hence maximum weld
- strength & tensile strength.

REFERENCES:

[1] Ganesh M, Praba Rajathi R, “EXPERIMENTAL STUDY ON ULTRASONIC WELDING OF ALUMINUM SHEET TO COPPER SHEET”, International Journal of Research in Engineering and Technology, 2013, p-161.

[2] Johns, J., DePrisco, C., “The Application of Ultrasonic Energy to Cold Welding of Metals”, Research report, Aero projects Inc. November, 1953, pp. 53-77.

[3] Edgar de Vries (FH), “Mechanics and Mechanisms of Ultrasonic Metal Welding”, The Ohio State University, 2004, p-10 [4] de Vries, E., “Development of ultrasonic welding process for stamped 6000 series Aluminum”, Diploma Thesis, University of Applied Science, Emden, 2000, p-79.

[5] Beyer, W., The bonding process in the ultrasonic welding of metals, Schweisstechnik, Jan. 1969, pp. 16-20.

[6] Gutensohn, M., Wagner, G., Eifler, D., Reduction of the Adherence of Aluminum On Ultrasonic Welding Tools, University of Kaiserslautern, 2004, pp. 78 -90.

[7] Wodara, J., Sporckenbach, D., “Choice of suitable measurement parameters for the control of ultrasonic welding processes”, Wissenschaftliche Zeitschrift der Technischen Hochschule Otto von Guericke Magdeburg, 1985, v.29, n. 8, pp. 77-88.

[8] Rozenberg, L., Mitskevich, A., “Ultrasonic welding of Metals”, Physical Principles Of Ultrasonic Technology, V.1, Part 2, Acoustic Institute Academy of Sciences of the USSR, Moscow, USSR, 1970, pp. 37-45.